

Average PER Prediction Based on Statistical CSI for SC-FDE Systems

Xavier Leturc
Thales SIX GTS France
4 avenue des Louvresses
92622 Gennevilliers Cedex
xavier.leturc@thalesgroup.com

Christophe J. Le Martret
Thales SIX GTS France
4 avenue des Louvresses
92622 Gennevilliers Cedex
christophe.le_martret@thalesgroup.com

Abstract—In this paper, we propose a method to predict the average packet error rate (PER) of a coded single carrier frequency domain equalization (SC-FDE) transmission scheme after minimum mean square error (MMSE) equalization when statistical channel state information (SCSI) is available. We assume that the encoded bits are spread over several blocks (which may correspond to a frequency hopping system for instance) which are transmitted under independent multipath random fading channel realizations. The PER prediction technique used here is based on the effective SNR mapping approach that gathers the signal to noise ratios (SNR)s of the different blocks into one single value. The novelty of this contribution resides in the fact that we propose a new expression for the effective SNR that allows us to approximate its statistical distribution with a beta random variable whose parameters depend on the SCSI. This approach enables us to compute the PER prediction with a lower complexity than the one required by conventional approaches. Moreover, we show by simulations that the accuracy of our solution is very close to the conventional ones, typically within 1 dB of error for PER of the order of 10^{-2} .

I. INTRODUCTION

Packet error rate (PER) prediction of communication links is of great interest in wireless communications either for system design and performance analysis [1], or link adaptation [2].

In the case of multicarrier schemes such as orthogonal frequency division multiplexing (OFDM) and single carrier frequency domain equalization (SC-FDE) used in recent systems such as the long term evolution (LTE) standard, the PER prediction is performed using the well-known effective signal to noise ratio mapping (ESM) method [3]. Indeed, for these schemes, the time-domain multipath impulse response of the channel is transformed into a single-tap in the frequency domain on each subcarrier which can thus be equalized with low complexity. As a consequence, each subcarrier has a specific signal to noise ratio (SNR). The ESM allows to estimate an equivalent SNR, called *effective SNR*, which would lead to the same PER when transmitting in an additive white Gaussian noise (AWGN) channel with the same modulation and coding scheme (MCS).

The most common techniques to compute the effective SNR are the mutual information effective SNR mapping (MIESM) and the exponential effective SNR mapping (EESM) [3]. These techniques enable to predict instantaneous PER assuming that the instantaneous channel state information (CSI) is available,

i.e. the instantaneous channel impulse response is known or estimated.

However, there exist contexts in which we only know the channel power delay profile (PDP) instead of its instantaneous realizations, which will be referred to as statistical CSI (SCSI) in the sequel. This is the case for instance for link adaptation in ad hoc networks [4], [5], or in assisted device-to-device networks [6]. In these cases, computing the predicted average PER requires the knowledge of the effective post-equalization SNR distribution. Previous works in the OFDM case with EESM are for instance [2] for throughput prediction and [7] for PER prediction. In [2], the authors approximate the statistical distribution of the effective SNR of EESM by a beta distribution whereas in [7] this statistical distribution is obtained through numerical convolution. To the best of our knowledge, predicting the PER for SC-FDE schemes with minimum mean square error (MMSE) equalization in the SCSI context has never been addressed so far in the literature. The most relevant work is in [8] where the author analyzes the outage performance of soft-cancellation frequency-domain minimum-mean-square error turbo equalization in a serially concatenated coded modulation scheme over frequency-selective Rayleigh fading channels from the PDP. In this work, the distribution of the post-MMSE-equalization SNR is modeled by a normal distribution.

In this paper, we propose a procedure to predict the average PER for MMSE equalized SC-FDE systems when only SCSI is available. The procedure is based upon the ESM technique for which we propose a new effective SNR expression. Moreover we also compare the complexity of the proposed method with the one that would be required using the conventional MIESM and EESM ones.

The rest of the paper is organized as follows. In Section II, we detail the model of the system. In Section III, we derive the proposed PER prediction procedure. In Section IV, we present numerical results to assess the proposed procedure accuracy. Finally, in Section V, we draw concluding remarks.

II. SYSTEM MODEL

The information packet to be transmitted is composed of K_B bits which are passed through a bit interleaved coded modulator, resulting in a stream of K_S modulated symbols,

denoted as $\mathbf{s} := [s_1, \dots, s_{K_S}]$ and referred to as the encoded codeword in the rest of the paper. This encoded codeword is then divided into N_B blocks of size n : $\mathbf{s} := [\tilde{\mathbf{s}}_1, \dots, \tilde{\mathbf{s}}_{N_B}]$ where $\tilde{\mathbf{s}}_i$ is a $(1 \times n)$ vector, and each block is transmitted in a different SC-FDE symbol. We assume that the SC-FDE symbols are transmitted over a bandwidth B that is divided into N_c subcarriers. The transmission is done over a subset of n subcarriers denoted by $I = \{I_1, \dots, I_n\}$, where I_k , $1 \leq k \leq n$, is the subcarrier index with $1 \leq I_k \leq N_c$. The i th transmit SC-FDE symbol carrying $\tilde{\mathbf{s}}_i$ is obtained by adding a cyclic prefix (CP) to the following $(N_c \times 1)$ vector: $\mathbf{x}_i := \sqrt{P} \mathbf{F}_{N_c}^H \mathbf{M}^T \mathbf{S}_i^T$, where $(\cdot)^T$ (resp. $(\cdot)^H$) stands for the transpose (resp. transpose conjugate) operator, P is the transmit power, \mathbf{F}_k is the normalized $(k \times k)$ discrete Fourier transform (DFT) matrix, $\mathbf{S}_i := \mathbf{F}_n \tilde{\mathbf{s}}_i^T$, and \mathbf{M} is the $(n \times N_c)$ demapping matrix, whose (k, ℓ) th entry is equal to 1 if $\ell = I_k$ and is equal to 0 otherwise.

The signal is transmitted through a frequency-selective random fading channel, whose sampled impulse response is noted by the $(L \times 1)$ vector $\mathbf{h}_i = [h_i(0), \dots, h_i(L-1)]^T$, where L is the length of the channel. We assume that $\mathbf{h}_i \sim \mathcal{CN}(\mathbf{0}, \mathbf{\Sigma})$, where $\mathcal{CN}(\mathbf{0}, \mathbf{\Sigma})$ stands for the complex Gaussian distribution with $\mathbf{0}$ mean and covariance matrix $\mathbf{\Sigma} := \text{diag}_{L \times L}(2\sigma_0^2, \dots, 2\sigma_{L-1}^2)$. We further assume that the channel impulse response changes independently between two consecutive SC-FDE symbols, i.e., $\mathbb{E}[\mathbf{h}_i \mathbf{h}_j^H] = \mathbf{0}$ if $i \neq j$.

When receiving the i th SC-FDE symbol, the receiver discards the CP, performs the size N_c DFT of the resulting signal, and demaps the samples of interest by multiplying resulting signal with the demapping matrix \mathbf{M} . After these operations, the received j samples of the i th block can be expressed as:

$$Y_i(j) = \sqrt{P} H_i(j) S_i(j) + W_i(j), \quad j = 1, \dots, n, \quad (1)$$

where $H_i(j)$ is the I_j th element of the size N_c DFT of \mathbf{h}_i , $S_i(j)$ is the j th element of \mathbf{S}_i , and $W_i(j)$ is a circularly symmetric white Gaussian noise with known variance $2\sigma_n^2$. It is worth noticing that $H_i(j) \sim \mathcal{CN}(0, 2\sigma_H^2)$, with $2\sigma_H^2 = \text{Tr}(\mathbf{\Sigma})$.

The received signal expressed in (1) is passed through a MMSE equalizer and $\hat{S}_i(j)$, the estimated value of $S_i(j)$, is thus given by $\hat{S}_i(j) = \sqrt{P} \hat{H}_i(j) / (P |H_i(j)|^2 + 2\sigma_n^2) Y_i(j)$. The receiver then computes the size n inverse DFT of the estimates $\hat{S}_i(j)$, $j = 1, \dots, n$, and carries out a soft-demapping on the resulting estimated symbols. To do so, the receiver needs to compute the post-MMSE-equalization SNR of the i th block. It is proved in [9] that this post-MMSE-equalization SNR is the same on all the subcarriers of the i th block, and is equal to:

$$\gamma_i(P) = \frac{a_i(P)}{1 - a_i(P)}, \quad (2)$$

where $a_i(P)$ is the signal-plus-interference-plus-noise ratio (SSINR) of the i th block, which can be expressed as:

$$a_i(P) := \frac{1}{n} \sum_{j=1}^n \frac{P |H_i(j)|^2}{P |H_i(j)|^2 + 2\sigma_n^2}. \quad (3)$$

Finally, once the N_B blocks have been received and demapped, the resulting log-likelihood ratios are deinterleaved and provided as an input to the decoder. The average PER of such a system is the probability of decoding the encoded codeword \mathbf{s} with error. Notice that (3) corresponds to one single realization of the channel \mathbf{h}_i and that in this paper we are looking to performance prediction in the SCSI context when only the statistics of \mathbf{h}_i are known, i.e. the channel covariance matrix $\mathbf{\Sigma}$ is available. In practice, this matrix can be estimated using the method derived in [10].

III. PROPOSED PER PREDICTION METHODOLOGY

A. Average PER expression using the ESM with statistical CSI

Let $q_A(\gamma(P))$ denote the instantaneous PER of the system described in Section II under the AWGN channel for a given MCS, with $\gamma(P) := [\gamma_1(P), \dots, \gamma_{N_B}(P)]$, the vector collecting all the block SNRs experimented on the different transmitted blocks. The average PER, denoted by $q(P)$, is defined as the expectation of the instantaneous PER with respect to $\gamma(P)$ ¹:

$$q(P) = \mathbb{E}_{\gamma(P)} [q_A(\gamma(P))]. \quad (4)$$

Computing the exact value of the expectation in (4) is analytically intractable. Using the ESM approach allows to simplify the problem by replacing the computation of (4) by the following approximation:

$$\tilde{q}(P) = \mathbb{E}_{\gamma_{\text{eff}}(P)} [q_A(\gamma_{\text{eff}}(P))], \quad (5)$$

where $\gamma_{\text{eff}}(P)$ is the effective SNR computed from $\gamma(P)$ thanks to the ESM. Let $p_{\gamma_{\text{eff}}(P)}(x)$ denote the probability density function (PDF) of $\gamma_{\text{eff}}(P)$. Then, (5) can be equivalently written as:

$$\tilde{q}(P) = \int_0^{+\infty} p_{\gamma_{\text{eff}}(P)}(x) q_A(x) dx. \quad (6)$$

Thus, in order to compute (6), we need to know both $p_{\gamma_{\text{eff}}(P)}$ and $q_A(x)$.

In practice, $q_A(x)$ is estimated by simulating the communication scheme in AWGN or can be approximated by a parametric function. For the density $p_{\gamma_{\text{eff}}(P)}$, its expression depends on the $\gamma_{\text{eff}}(P)$ function selected to compute the effective SNR. For instance, for the MIESM technique, the expression is given by:

$$\gamma_{\text{eff}}^{\text{MI}}(P) = \alpha_1 J^{-1} \left(\frac{1}{N_B} \sum_{i=1}^{N_B} J \left(\frac{\gamma_i(P)}{\alpha_2} \right) \right) \quad (7)$$

where $J(\cdot)$ is the mutual information, α_i , $i = 1, 2$, are fitting coefficients adapted to the MCS, and $J^{-1}(\cdot)$ is the inverse of $J(\cdot)$ with respect to the composition. The mutual information cannot be expressed in closed form and needs to be evaluated through simulations for each considered modulation and tabulated. In the EESM case, the expression of $\gamma_{\text{eff}}^{\text{E}}(P)$ is similar to (7) where $J(x)$ is replaced by $\exp(-x)$ and $J^{-1}(x)$ by $-\log(x)$.

¹By abuse of notation we use the same names to figure the random variables and their realizations.

B. New effective SNR expression

In this paper, we propose an alternative definition of the effective SNR based upon the SSINR values (3) and name it as: SSINR effective SNR mapping (SSESM). Its expression is given by:

$$\gamma_{\text{eff}}^{\text{SS}}(P) := \frac{\bar{a}(P)}{1 - \bar{a}(P)}, \quad (8)$$

with

$$\bar{a}(P) := \frac{1}{N_B} \sum_{i=1}^{N_B} a_i(P). \quad (9)$$

The SSESM expression (8) has the same form as the SNR per block (2) where the $a_i(P)$ value is replaced by the average value of the SSINR over all the blocks. Intuitively, defining $\bar{a}(P)$ as (9) corresponds to assuming that the whole encoded codeword is sent on a single SC-FDE symbol which experiments a channel whose frequency response is the concatenation of the channels frequency response experimented by the actual SC-FDE symbols. It is worth noting that although (8) is introduced in the SCSI context, it can be used likewise with instantaneous CSI for PER prediction in the the SC-FDE context, the same way as it is done when using MIESM or EESM.

This new expression will be shown to allow a less complex implementation than the conventional ones (discussed in Section III-E) while keeping similar accuracy (validation is provided in Section IV).

C. PER prediction

To evaluate the PER from (6), we first resort to the approximation used in [11] which consists in approximating $q_A(x)$ by $\tilde{q}_A(x)$ as follows:

$$\tilde{q}_A(x) := \begin{cases} 1 & \text{if } x \leq \gamma_{\text{th}}, \\ 0 & \text{if } x > \gamma_{\text{th}}, \end{cases} \quad (10)$$

where γ_{th} is a SNR threshold which depends on the MCS. It is obtained by performing PER simulations in the AWGN channel for a given MCS and numerically evaluating the γ_{th} value which best fits (10). It is important to notice at this point that γ_{th} does not depend on the effective SNR expression and thus is common to all ESM methods as long as (10) is used.

Replacing $q_A(x)$ by $\tilde{q}_A(x)$ in (6), we immediately get:

$$\tilde{q}(P) = F_{\gamma_{\text{eff}}(P)}(\gamma_{\text{th}}), \quad (11)$$

where $F_{\gamma_{\text{eff}}(P)}(\gamma_{\text{th}}) = \Pr(\gamma_{\text{eff}}(P) \leq \gamma_{\text{th}})$ is the cumulative distribution function (CDF) of $\gamma_{\text{eff}}(P)$. Applied to our new effective SNR mapping expression (8), we get from (9):

$$\begin{aligned} F_{\gamma_{\text{eff}}^{\text{SS}}(P)}(\gamma_{\text{th}}) &= \Pr\left(\frac{\bar{a}(P)}{1 - \bar{a}(P)} \leq \gamma_{\text{th}}\right) \\ &= \Pr\left(\bar{a}(P) \leq \frac{\gamma_{\text{th}}}{1 + \gamma_{\text{th}}}\right), \end{aligned}$$

leading to:

$$F_{\gamma_{\text{eff}}^{\text{SS}}(P)}(\gamma_{\text{th}}) = F_{\bar{a}(P)}\left(\frac{\gamma_{\text{th}}}{1 + \gamma_{\text{th}}}\right), \quad (12)$$

where $F_{\bar{a}(P)}(x)$ is the CDF of $\bar{a}(P)$. As is will be exposed in Section III-D, we propose to approximate the PDF of $\bar{a}(P)$ by a beta distribution with parameters α and β , which leads to:

$$F_{\bar{a}(P)}(x) \approx I_x(\alpha, \beta), \quad (13)$$

where $I_x(\alpha, \beta)$ is the regularized incomplete beta function [12]. From (13), (12) and (11), we finally get:

$$\tilde{q}(P) \approx I_{\frac{\gamma_{\text{th}}}{1 + \gamma_{\text{th}}}}(\alpha, \beta). \quad (14)$$

D. Statistics of the post-MMSE-equalization SNRs

As stated in Section III-C, we propose to approximate the PDF of $\bar{a}(P)$ in (9) by a beta distribution. The reason for such a choice is the following one. First, we can see from the expression (3) that $a_i(P)$ take its values in $[0, 1]$. As a consequence, (9) can be interpreted as the sum of identically distributed random variables with finite support. Thus, using the same approach as in [2], $\bar{a}(P)$ can be approximated by a beta distribution. In this approach, the evaluation of the α and β parameters is performed through a moment-matching technique at order two. If Y denotes a random variable following beta distribution with parameters α and β , we compute these parameters such that the expectation and variance of $\bar{a}(P)$ and Y are equal, i.e., $\mathbb{E}[\bar{a}(P)] = \mathbb{E}[Y]$, and $\text{Var}[\bar{a}(P)] = \text{Var}[Y]$. These two equalities yield [2]:

$$\alpha = \frac{\mathbb{E}[\bar{a}(P)]\mathcal{F}(P)}{\text{Var}[\bar{a}(P)]} \quad (15)$$

and

$$\beta = \frac{(1 - \mathbb{E}[\bar{a}(P)])\mathcal{F}(P)}{\text{Var}[\bar{a}(P)]} \quad (16)$$

with $\mathcal{F}(P) := (\mathbb{E}[\bar{a}(P)] - \mathbb{E}[\bar{a}(P)]^2 - \text{Var}[\bar{a}(P)])$. Evaluating (15) and (16) requires to compute $\mathbb{E}[\bar{a}(P)]$ and $\text{Var}[\bar{a}(P)]$. To do so, we take inspiration from the approach derived in [8] but applied in a different context to (9), leading to the following result.

Result 1. *The expectation and variance of $\bar{a}(P)$ can be written as:*

$$\mathbb{E}[\bar{a}(P)] = \frac{-2\sigma_n^2}{P2\sigma_H^2} e^{\frac{2\sigma_n^2}{P2\sigma_H^2}} E_1\left(\frac{2\sigma_n^2}{P2\sigma_H^2}\right) + 1, \quad (17)$$

$$\begin{aligned} \text{Var}[\bar{a}(P)] &= \frac{1}{N_B} \left(\frac{\mathcal{G}(P)}{n} - \right. \\ &\quad \left. (\mathbb{E}[\bar{a}(P)])^2 + \frac{2}{n^2} \sum_{j=1}^{n-1} (n-j)\lambda_j \right) \end{aligned} \quad (18)$$

where $E_1(\cdot)$ is the exponential integral function, and

$$\mathcal{G}(P) := 1 + \frac{\sigma_n^2}{P\sigma_H^2} \left(1 - e^{\frac{\sigma_n^2}{P\sigma_H^2}} E_1\left(\frac{\sigma_n^2}{P\sigma_H^2}\right) \left(\frac{\sigma_n^2}{P\sigma_H^2} + 2 \right) \right), \quad (19)$$

$$\lambda_j := \omega_{1,j} \sum_{k=0}^{+\infty} \frac{\omega_{2,j,k}}{4P^{2k+2}} \left[(-1)^{k+1} (2\sigma_n^2)^{k+1} e^{\frac{2\sigma_n^2}{P\omega_{3,j,k}}} E_1 \left(\frac{\sigma_n^2}{P\omega_{3,j,k}} \right) + \sum_{i=1}^{k+1} (i-1)! (-2\sigma_n^2)^{k+1-i} (P\omega_{3,j,k})^i \right], \quad (20)$$

with $\omega_{1,j} := 1/(\sigma_H^4(1 - \rho_j))$, $\omega_{2,j,k} := (2\sqrt{\rho_j})^{2k}/(4^k(k!)^2(\omega_{3,j,k})^{2k})$, $\omega_{3,j,k} := (1 - \rho_j)2\sigma_H^2$, and $\rho_j := \text{Cov}(|H_i(1)|^2, |H_i(j+1)|^2)/\text{Var}(|H_i(1)|^2)$.

In the following Result 2 whose proof is omitted due to space limitation, we derive the closed form expression of ρ_j as a function of the PDP, i.e., the diagonal elements of the channel covariance matrix Σ .

Result 2. *The parameters ρ_i can be expressed as:*

$$\rho_j = 4 \sum_{\ell=0}^{L-1} \sigma_\ell^4 + 8 \sum_{\substack{0 \leq \ell < \ell' \\ \ell' \leq L-1}} \sigma_\ell^2 \sigma_{\ell'}^2 \cos \left(2\pi \frac{e_j}{N_c} (\ell - \ell') \right) \quad (21)$$

where e_j is the difference between the first and the $(j+1)$ th subcarrier indexes, i.e., $e_j = I_{j+1} - I_1$.

Thus, the moment-matching identification of α and β is done by computing first $\mathbb{E}[\bar{a}(P)]$ and $\text{Var}[\bar{a}(P)]$ using (17) and (18) thanks to (19), (20) and (21). Second, by inserting the computed values of $\mathbb{E}[\bar{a}(P)]$ and $\text{Var}[\bar{a}(P)]$ in (15) and (16). It is worth noting that the α and β values depend on the PDP and thus have to be updated according to the PDP evolution in time with respect to the changes of the propagation environment.

E. Complexity analysis

In this section, we compare the complexity of our proposed average PER prediction solution based on SSESMS against the conventional ones based on MIESM and EESM. It is important to notice that neither the MIESM nor EESM have been described in the literature in the context of PER prediction with SCSi in the case SC-FDE with MMSE equalization. Thus, this section also gives an overall description of what could be the implementation of these two alternative approaches.

First, it is important to notice that the derivations provided in Section III-C work for all the methods up to (11), which states that the average PER is expressed as a function of the CDF of the effective SNR. Thus the evaluation of γ_{th} is common to all the methods. It turns out that thanks to the simple expression of $\gamma_{\text{eff}}^{\text{SS}}(P)$ we get a closed form expression of the approximated average PER by modeling the PDF of $\bar{a}(P)$ by a beta distribution. This modeling requires a moment-matching procedure to estimate the beta distribution parameters.

For the MIESM or EESM, the evaluation of the CDF of the effective SNR is more complex since it requires to evaluate the PDF of $\sum_{i=1}^{N_B} J \left(\frac{\gamma_i(P)}{\alpha_2} \right)$. To do so, a first step to find the PDF of $\gamma_i(P)$ is needed. This can be done using a moment-matching approach as we have proposed for our method by approximating the $a_i(P)$ with a beta random variable and deducing the distribution of $\gamma_i(P)$ in closed

form from (2). Thus regarding the complexity, all the methods require a moment-matching phase. Now, calculating the PDF of $\sum_{i=1}^{N_B} J \left(\frac{\gamma_i(P)}{\alpha_2} \right)$ is intractable in closed form and needs to be evaluated using multiple discrete numerical convolutions of the sampled PDF of $J \left(\frac{\gamma_i(P)}{\alpha_2} \right)$, even if the PDF can be written in closed form. Indeed, for the EESM method, computing the PDF of $\exp - \left(\frac{\gamma_i(P)}{\alpha_2} \right)$ can be done in closed form. However, since the beta law is used to model $a_i(P)$, then the resulting distribution of $\exp - \left(\frac{\gamma_i(P)}{\alpha_2} \right)$ involves the beta distribution as well, which can present discontinuities around zero, requiring some tricks to process the numerical evaluation of the convolutions [7]. Last, it is worth noting that the evaluation of the PDF of the effective SNR needs to be computed each time the PDP changes.

Thus we can conclude that computing the average PER prediction using MIESM and EESM methods requires extra numerical processing calculations (multiple numerical convolutions) which have to be performed each time the PDP evolves compared to our method. As a consequence, we can state that the proposed procedure based on SSESMS is less complex than the MIESM and EESM. This is an important point for distributed networks where the resource allocation algorithms are embedded in the mobile nodes which have less computational capabilities than fixed infrastructure equipment.

IV. NUMERICAL RESULTS

In this Section, we perform simulations aiming at *i*) comparing the proposed solution SSESMS with the conventional MIESM in terms of PER prediction when full CSI is available, and *ii*) evaluating the accuracy of the proposed average PER prediction methodology when only SCSi is available.

A. Setup

1) *Implemented MCSs:* We implemented the LDPC code of the 5G [13], along with the following three MCSs: MCS1, which uses the QPSK modulation with code rate 1/2, MCS2, which uses the 8PSK modulation with code rate 2/3, and MCS3, which uses the 16APSK modulation with code rate 3/4. The number of uncoded bits for each of these MCSs is chosen such that the number of modulated symbol in the encoded codeword is the same for each MCS and is equal to 1,000. In Table I, we provide the number of uncoded bits for each MCS, along with the values of γ_{th} we used in the PER approximation (14).

TABLE I: Number of uncoded bits and values of the threshold γ_{th} for the three implemented MCSs.

	MCS1	MCS2	MCS3
Uncoded bits	1,000	2,000	3,000
γ_{th} (dB)	1.25	6.5	10

2) *Channel models:* We considered two PDPs for the channel:

- i*) **Uniform Channel (UC):** a uniform PDP channel with $L = 2$ and $L = 6$ taps.

ii) **Proakis Like Channel (PLC)** [14]: a channel with $L = 3$ and $L = 7$ taps, whose covariance matrix is provided by $\Sigma = 1/4 \times \text{diag}_{3 \times 3}(1, 2, 1)$ and $\Sigma = 1/16 \times \text{diag}_{7 \times 7}(1, 2, 3, 4, 3, 2, 1)$ for $L = 3$ and $L = 7$, respectively

3) **Assumptions on the allocated subcarriers**: We assume that the bandwidth is divided into $N_c = 2,048$ subcarriers numbered from 1 to 2,048, and we implemented the following three cases regarding the allocated subcarriers.

i) **Full Channels (FC)**: the 1024 central subcarriers are allocated for communications, i.e., $I = (513, 514, \dots, 1536)$, and thus $N_B = 1$.

ii) **Half Channels (HC)**: 512 subcarriers are allocated. These subcarriers are the same as in the FC case down-sampled by a factor two i.e., $I = (513, 515, \dots, 1536)$, and thus $N_B = 2$.

iii) **Quarter Channels (QC)**: 256 subcarriers are allocated. These subcarriers are the same as in the FC case down-samples by a factor four i.e., $I = (513, 517, \dots, 1536)$, and thus $N_B = 4$.

B. Comparing SSESIM with MIESM with full CSI

In this section, we compare the performance of MIESM and SSESIM in terms of PER prediction when full CSI is available. Indeed, although the procedure developed in this paper aims to predict PER with SCSIM, SSESIM provided in (8) also enables SNR mapping when full CSI is available and thus it is of interest to assess its accuracy to predict PER with full CSI as well. To do so, we first perform simulations (not shown in this paper) to tabulate the PER for the three considered MCSs under the AWGN channel. Second, we perform simulations under the considered fading channels in the HC and QC cases. More precisely, for a given average SNR we transmit 10^4 encoded codewords, each codeword being segmented into N_B blocks (i.e., SC-FDE symbols) and each block experiments an independent random fading channel realization generated according to the considered PDP. At the reception of each encoded codeword, we compute the effective post-MMSE-equalization SNR considering that the channel is perfectly known using both i) the conventional MIESM procedure provided by (7) where we set $\alpha_i = 1$, $i = 1, 2$, and ii) our proposed procedure provided by (8) along with (9) and (3). Then, we predict the PER using these effective SNRs values by reading the corresponding error probability under the AWGN channel in the look-up table.

In Fig. 1 and Fig. 2, we plot the PER obtained by simulation and predicted PER using MIESM and SSESIM versus the average SNR for the three considered MCSs under the UC (top) and the PLC (bottom) in the HC and QC configurations, respectively. We can observe that the proposed SSESIM methodology enables very accurate PER prediction for the MCS1, indeed, the PER curves obtained by simulation are almost superimposed with the prediction obtained using SSESIM. We can also see that despite SSESIM is slightly less accurate for MCS2, the maximal deviation does not exceed 0.75 dB. Last, we can observe that SSESIM enables accurate

PER prediction for MCS3, in fact, it is even more accurate than MIESM.

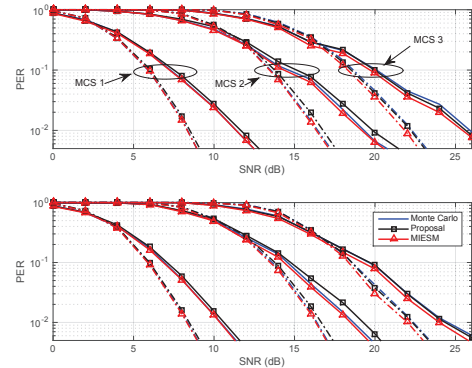


Fig. 1: PER obtained by simulation and predicted PER using MIESM and SSESIM the average SNR under the UC (top) and the PLC (bottom) in the HC configuration. Solid lines: $L = 2$ in the UC and $L = 3$ in the PLC, dashed lines: $L = 6$ in the UC and $L = 7$ in the PLC.

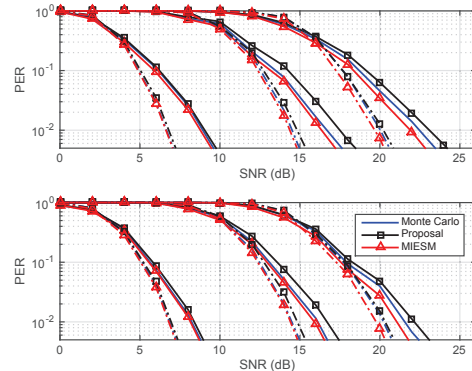


Fig. 2: PER obtained by simulation and predicted PER using MIESM and SSESIM versus the average SNR under the UC (top) and the PLC (bottom) in the QC configuration. Solid lines: $L = 2$ in the UC and $L = 3$ in the PLC, dashed lines: $L = 6$ in the UC and $L = 7$ in the PLC.

C. Accuracy of SSESIM with statistical CSI

In this section, we assess the accuracy of the proposed average PER prediction methodology when SCSIM is available. To do so, we perform the same Monte Carlo simulations than in Section IV-B to obtain the theoretical average PER curves. Then, we compute the predicted PER using (12) with the values of γ_{th} provided in Table I.

In Figs. 3 to 5, we plot the PER obtained by simulations and the predicted PER obtained using the proposed methodology under the UC (top) and the PLC (bottom) versus the SNR for MCS1, MCS2, and MCS3, respectively for the FC and the QC configurations. We can observe that the maximum deviation is less than 1 dB for PER of the order of 10^{-2} .

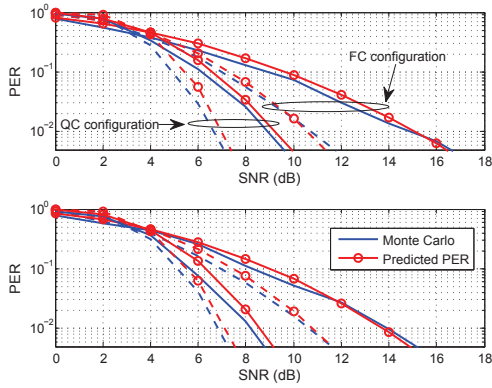


Fig. 3: PER obtained by simulation and using our proposed prediction method versus the average SNR under the UC (top) and the PLC (bottom) for MCS1. Solid lines: $L = 2$ in the UC and $L = 3$ in the PLC, dashed lines: $L = 6$ in the UC and $L = 7$ in the PLC.

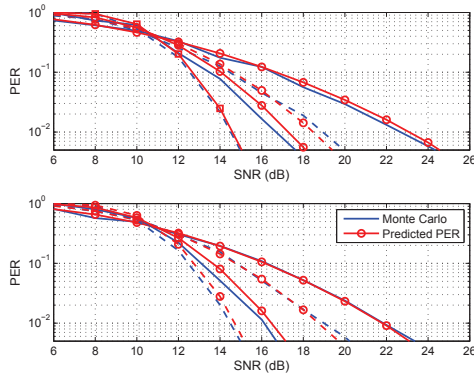


Fig. 4: PER obtained by simulation and using our proposed prediction method versus the average SNR under the UC (top) and the PLC (bottom) for MCS2. Solid lines: $L = 2$ in the UC and $L = 3$ in the PLC, dashed lines: $L = 6$ in the UC and $L = 3$ in the PLC.

V. CONCLUSION

In this paper, we proposed a methodology to predict the average PER for coded SC-FDE systems using MMSE equalizer when SCS is available, based on the effective SNR mapping approach. The novelty of our approach is to introduce new post-equalization SNRs and effective SNR expressions which allow to approximate the effective SNR distribution by a beta distribution with low complexity compared to conventional methods. We assessed the accuracy of the proposed methodology through simulations and showed that it enables accurate PER prediction for PER down to 10^{-2} . Extensions of this work could be: *i*) taking into account other channel models such as the Rician one, and *ii*) use the proposed PER prediction methodology to perform resource allocation.

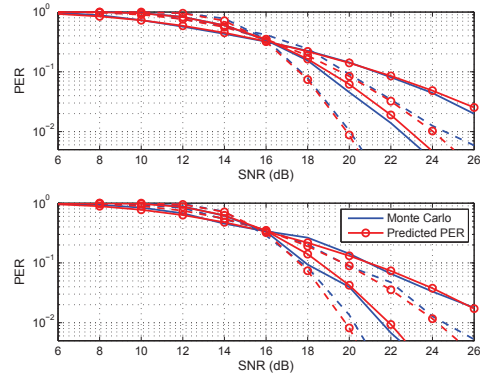


Fig. 5: PER obtained by simulation and using our proposed prediction method versus the average SNR under the UC (top) and the PLC (bottom) for MCS3. The solid lines stand for $L = 2$ in the UC and $L = 3$ in the PLC, whereas the dashed lines stand for $L = 6$ in the UC and $L = 3$ in the PLC.

ACKNOWLEDGMENT

This research work was carried out in the framework of the MAENA EDA Project No B-1476-IAP4-GP.

REFERENCES

- [1] K. J. Kim, T. A. Khan, and P. V. Orlik, "Performance analysis of cooperative systems with unreliable backhauls and selection combining," *IEEE Trans. Veh. Technol.*, vol. 66, no. 3, pp. 2448–2461, 2017.
- [2] J. Francis and N. B. Mehta, "EESM-based link adaptation in point-to-point and multi-cell OFDM systems: Modeling and analysis," *IEEE Trans. Wireless Commun.*, vol. 13, no. 1, pp. 407–417, 2014.
- [3] K. Brueninghaus, D. Astely, T. Salzer, S. Visuri, A. Alexiou, S. Karger, and G.-A. Seraji, "Link performance models for system level simulations of broadband radio access systems," in *PIMRC*. IEEE, 2005.
- [4] X. Leturc, P. Ciblat, and C. J. Le Martret, "Energy efficient resource allocation for Type-I HARQ under the Rician channel," *IEEE Trans. Wireless Commun.*, vol. 18, no. 7, pp. 3739–3751, 2019.
- [5] M. Maaz, P. Mary, and M. Hélaré, "Energy minimization in HARQ-I relay-assisted networks with delay-limited users," *IEEE Trans. Veh. Technol.*, vol. 66, no. 8, pp. 6887–6898, 2017.
- [6] G. Fodor, E. Dahlman, G. Mildh, S. Parkvall, N. Reider, G. Mikls, and Z. Turnyi, "Design aspects of network assisted device-to-device communications," *IEEE Commun. Mag.*, vol. 50, no. 3, pp. 170–177, Mar. 2012.
- [7] J. Gaveau, C. J. Le Martret, and M. Assaad, "Grouping of subcarriers and effective SNR statistics in wideband OFDM systems using EESM," in *WiMob*, 2017, pp. 1–7.
- [8] M. Grossmann, "Outage performance analysis and code design for three-stage MMSE turbo equalization in frequency-selective Rayleigh fading channels," *IEEE Trans. Veh. Technol.*, vol. 60, no. 2, pp. 473–484, 2011.
- [9] D. Zanatta Filho, L. Féty, and M. Terré, "A hybrid single-carrier/multicarrier transmission scheme with power allocation," *EURASIP journal on wireless communications and networking*, no. 1, p. 168032, 2007.
- [10] Y. Kim and G. Im, "Pilot-symbol assisted power delay profile estimation for MIMO-OFDM systems," *IEEE Commun. Lett.*, vol. 16, no. 1, pp. 68–71, 2012.
- [11] I. Chatzigeorgiou, I. J. Wassell, and R. Carrasco, "On the frame error rate of transmission schemes on quasi-static fading channels," in *42nd Annual Conference on Information Sciences and Systems*, 2008.
- [12] I. S. Gradshteyn and I. M. Ryzhik, *Table of integrals, series, and products*. Academic press, 2014.
- [13] F. Hamidi-Sepéhr, A. Nimbalkar, and G. Ermolaev, "Analysis of 5G LDPC codes rate-matching design," in *IEEE 87th VTC Spring*, 2018.
- [14] J. G. Proakis and M. Salehi, *Digital communications*. McGraw-hill New York, 2001, vol. 4.